CHEMISTRY OF MATERIALS

Open Access

This article is licensed under CC-BY-NC-ND 4.0

pubs.acs.org/cm

Article

Polymer–Metal–Organic Frameworks (polyMOFs) Based on Tailor-Made Poly(alkenamer)s

Prantik Mondal, Debobroto Sensharma, and Seth M. Cohen*

Cite This: *Chem. Mater.* 2024, 36, 9696–9703

Read Online

ACCESS | Metrics & More | Article Recommendations | Supporting Information

ABSTRACT: Polymeric linkers used to construct porous, crystalline polymer–metal–organic frameworks (polyMOFs) are predominantly based on macromolecules with metal-coordinating ligand units (e.g., 1,4-benzenedicarboxylic acid, H_2bdc) included in the primary polymer backbone. Polymers with ligand units as pendants or dangling side chain substituents have been far less explored for the synthesis of polyMOFs, despite the fact that such systems may have distinct properties and could take advantage of a variety of chain polymerization methods. Prevailing reports are based on nonliving polymerized linkers with H_2bdc pendants that generated polyMOFs with key shortcomings in controlling the polymerization, tailoring polymeric linker composition and polyMOF properties, accessing porosity, etc. Herein, polymers containing H_2bdc units as pendants were designed and synthesized via controlled olefin-metathesis polymerization. These poly(alkenamer)s were subsequently assembled into porous, crystalline networks with an isoreticular MOF (IRMOF) lattice topology. These polymer architectures and polymerization methodologies provide access to the formation of polyMOFs with tailored characteristics, including controlled composition, narrow dispersity, and side chain functionalization.

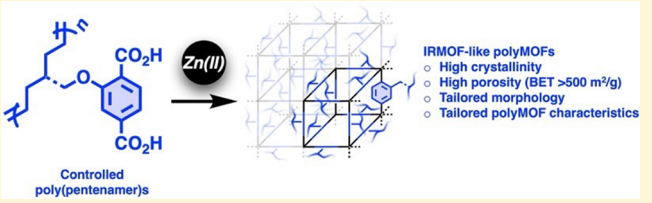

INTRODUCTION

Macromolecules containing ligating units (e.g., 1,4-benzenedicarboxylic acid and H_2bdc) in the polymer backbone have been almost exclusively used to generate polyMOFs (Figure 1). Synthesizing and designing these polymer ligands is somewhat limited by the type of monomers that can be accessed and the available methods for polymerization,[1] which may be one reason why the broader potential of polyMOFs has not yet been realized. Alternatively, a polymer with pendant or dangling ligating groups that are not part of the polymer backbone might allow for the design and access to a greater range of functional monomers and polymer ligands with more diverse chemical and physical properties using a vast library of chain polymerization methods.

Reports on the preparation of polyMOFs using polymeric linkers with pendant H_2bdc units are rare. Yazaki et al. assembled a polyMOF with an isoreticular MOF-5 (IRMOF-1) structure using a polymer ligand with H_2bdc side chain units and a poly(vinyl ether) backbone (Figure 1).[2] Solvothermal synthesis using the polymer ligand and zinc nitrate hexahydrate ($Zn(NO_3)_2{\cdot}6H_2O$) in DMF at 100 °C gave a crystalline polyMOF that was nonporous, as determined by dinitrogen (N_2) gas sorption analysis and Brunauer–Emmett–Teller (BET) surface area calculation (<1 m^2/g). The poly(vinyl ether)-based ligand was obtained via nonliving cationic polymerization that exhibited poor polymerization control, resulting in its broad polydispersity index ($Đ$) of 2.46. Cationic polymerization typically requires a rigorously anhydrous atmosphere, highly purified chemicals, and carefully designed cationic initiators to control and has limited functional group tolerance.[3−5] By contrast, controlled polymerizations not only result in narrow $Đ$ but also provide access to structurally tailored polymers with preferred architectures and functionalities.[6,7] As such, Johnson et al. employed free and controlled radical polymerization to design polyacrylamide-based linkers containing H_2bdc units as side chain substituents with broad and narrow $Đ$s, respectively. The nonliving, free radical polymerized ligand formed a crystalline polyMOF with Zn(II); however, these polymers required 1−3 equiv of free H_2bdc (per repeat unit of polymer with the H_2bdc pendant) as a supporting colinker that produced MOF/polyMOF hybrid materials (Figure 1).[8]

Poly(alkenamer)s are a broad group of polyolefins used in industrial and commercial applications due, in part, to their processability and physical robustness.[9−11] Ring-opening metathesis polymerization (ROMP) is a common approach to obtaining poly(alkenamer) materials. Metathesis catalysts for ROMP are typically based on Grubbs' ruthenium and Schrock's molybdenum complexes.[12] The remarkable stability, functional group tolerance, and low cost of the Grubbs'

Received: June 27, 2024
Revised: September 12, 2024
Accepted: September 13, 2024
Published: October 2, 2024

© 2024 The Authors. Published by American Chemical Society

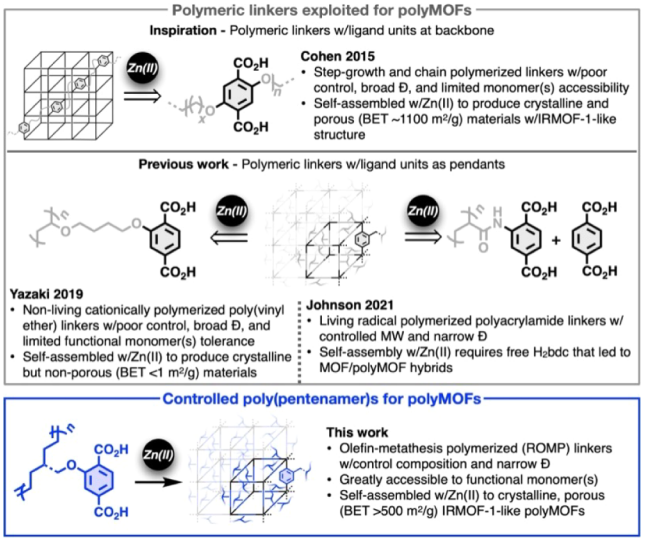

Figure 1. Top: overview of the types of polymeric linkers used for generating polyMOFs. Cohen et al.[16] synthesized the first crystalline, porous polyMOFs with IRMOF-like structures using polymers with ligand units in the primary backbone. Middle: Yazaki et al.[2] and Johnson et al.[8] utilized polymeric linkers with ligand units as pendant side chains based on poly(vinyl ether) and polyacrylamide backbones to prepare polyMOFs and MOF/polyMOF hybrids, respectively. Bottom: this work used a range of tailor-made poly(pentenamer)s (with controlled composition) to prepare polyMOFs with high crystallinity and porosity.

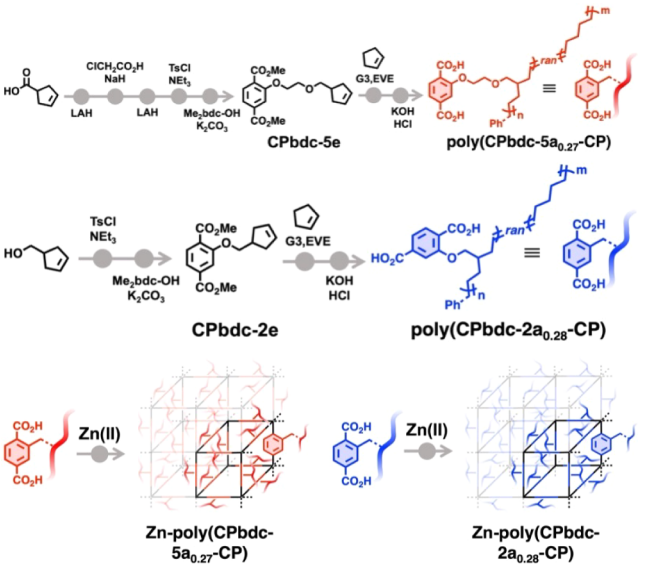

Figure 2. Top: scheme for the synthesis of poly(CPbdc-$5a_{0.27}$-CP). Middle: synthesis of poly(CPbdc-$2a_{0.28}$-CP). Bottom: synthesis of Zn-poly(CPbdc-$5a_{0.27}$-CP) (bottom-left) and Zn-poly(CPbdc-$2a_{0.28}$-CP) (bottom-right) under solvothermal conditions from poly(CPbdc-$5a_{0.27}$-CP) and poly(CPbdc-$2a_{0.28}$-CP), respectively.

ruthenium catalysts make ROMP an excellent method to polymerize a diverse range of functionalized olefins that cannot be synthesized using other chain growth polymerization approaches.[9,13−15] Due to its high initiation-to-propagation rate ratio, the Grubbs' third generation (G3) catalyst can produce highly controlled polymerizations of polyolefins, including poly(alkenamer)s, with narrow $Đ$ under mild reaction conditions.[14]

Herein, the cyclopentene-derived functional monomers were synthesized and polymerized via ROMP, followed by ester hydrolysis to obtain narrowly dispersed random poly(pentenamer)s with a controlled composition of H_2bdc pendant groups. These poly(pentenamer)s were subsequently assembled with Zn(II) into crystalline, porous polyMOFs with IRMOF-like structure types, as characterized by powder X-ray diffraction (PXRD), scanning electron microscopy (SEM), N_2 gas sorption, and BET surface area measurement. The percentage of H_2bdc repeating units in the polymer, the polyMOF synthetic conditions, and side chain or spacer lengths of the repeating units containing H_2bdc pendants (i.e., the length between the poly(pentenamer) backbone and the H_2bdc moiety; Figures 1 and 2) influenced the degree of crystallinity, porosity, and morphology of the resultant polyMOFs. To the best of our knowledge, no reports exist using ROMP to design narrowly dispersed polymeric ligands with a controlled composition of H_2bdc pendant groups to access polyMOFs and tailor the polyMOF characteristics.

EXPERIMENTAL METHODS

Materials. Starting materials, solvents, and gases were obtained from commercial suppliers (Combi-Blocks, Sigma-Aldrich, Alfa Aesar, TCI, Cambridge Isotope Laboratories Inc., etc.) and used without further purification unless otherwise noted. All organic molecules were synthesized using standard Schlenk techniques (see the Supporting Information for complete synthesis and characterization details). Solvents were dried under activated 4 Å molecular sieves before use. Dimethyl-2-hydroxyterephthalate was synthesized according to the literature procedure.[17] All of the synthesized monomers and polymers were stored under air-free conditions and used within a week after their synthesis.

Polymer Synthesis. *Poly(CPbdc-$5a_{0.27}$-CP).* An oven-dried 10 mL round-bottom flask was equipped with a magnetic stir bar, charged with CPbdc-5e (0.255 g, 0.76 mmol, 200 equiv), placed into an ice bath (at 0 °C), and stirred at ∼250 rpm to which cyclopentene (CP, 50.4 μL, 0.57 mmol, 150 equiv) was added, and sealed with a silicon septum. After 1 min, the Grubbs third generation (G3) catalyst (3.3 mg, 3.8 μmol, 1 equiv) was added as a solid by opening the seal of the flask and immediately capping it. The catalyst was miscible with the monomeric mixture. The solution was stirred at 0 °C and became viscous after 20 min. After 60 min, the reaction was quenched by adding 0.4 mL of cold ethyl vinyl ether and 0.4 mL of CH_2Cl_2 to solubilize the polymer. It took ∼5−10 min to dissolve the material, which was achieved by manual vortexing and gentle shaking in an ice bath. Once the polymer dissolved, the solution was stirred for another 15 min at 0 °C. To the viscous solution, 35 mL of cold MeOH was added to a 50 mL Falcon tube, and the resulting gummy precipitate was then washed with (3 × 20 mL) cold MeOH. Next, the polymer was redissolved and reprecipitated three times by dissolving the polymer in 0.2 mL of CH_2Cl_2 in a sealed Falcon tube, precipitating with 35 mL of MeOH, and washing with (3 × 20 mL) MeOH. The resulting polyester polymer, poly(CPbdc-$5e_{0.27}$-CP), was dried at room temperature under a vacuum (overnight, 16 h) and immediately used for the next step. Yield: 32 mg (16%). Figure S6 shows a pictorial illustration of the experimental setup of this polymerization.

To hydrolyze the polyester, an oven-dried 10 mL round-bottom flask was equipped with a magnetic stir bar and

https://doi.org/10.1021/acs.chemmater.4c01794
Chem. Mater. 2024, 36, 9696−9703

charged with 30 mg of poly(CPbdc-5e$_{0.27}$-CP) and dissolved in 2 mL of THF, to which 2 mL of aqueous KOH solution (0.45 g of KOH) was added. The biphasic system was stirred at ∼1000 rpm at room temperature under argon for 24 h. The THF solvent was removed under reduced pressure to obtain the alkaline aqueous layer, which was acidified (to pH = 1) with a dropwise addition of 1.5 M HCl to get a white precipitate. The residue was collected by centrifugation, washed with (3 × 40 mL) distilled water and (2 × 40 mL) MeOH, and dried for 24 h under a vacuum at room temperature to obtain the final product as faded brown solids. Yield: 27 mg (91%).

poly(CPbdc-2a$_{0.28}$-CP). An oven-dried 10 mL round-bottom flask was equipped with a magnetic stir bar, charged with CPbdc-2e (0.255 g, 0.87 mmol, 200 equiv), placed into an ice bath (at 0 °C), and stirred at ∼250 rpm, to which CP (50.4 μL, 0.57 mmol, 130 equiv) was added, and sealed with a silicon septum. After 1 min, the G3 catalyst (3.9 mg, 4.4 μmol, 1 equiv) was added as solids by opening the seal of the flask and immediately capping it. The catalyst was found to be miscible with the monomeric mixture. The solution was stirred at 0 °C and became viscous after 20 min. After 60 min, the reaction was quenched by adding 0.4 mL of cold ethyl vinyl ether and 0.4 mL of CH_2Cl_2 to solubilize the polymer. Once the polymer dissolved, the solution was stirred for another 15 min at 0 °C. To the viscous solution, 35 mL of cold MeOH was added to a 50 mL Falcon tube, and the resulting gummy precipitate was then washed with (3 × 20 mL) cold MeOH. Next, the polymer was redissolved and reprecipitated three times by dissolving the polymer in 0.2 mL of CH_2Cl_2 in a sealed Falcon tube, precipitating with 35 mL of MeOH, and washing with (3 × 20 mL) MeOH. Finally, the polyester polymer, was dried at room temperature under a vacuum (overnight, 16 h) and immediately used for the next step. Yield: 42 mg (18%).

To hydrolyze the polyester, an oven-dried 10 mL round-bottom flask was equipped with a magnetic stir bar and charged with 35 mg of poly(CPbdc-2e$_{0.28}$-CP) and dissolved in 2 mL of THF, to which 2 mL of aqueous KOH solution (0.53 g of KOH) was added. The biphasic system was stirred at ∼1000 rpm at room temperature under argon for 24 h. The THF solvent was removed under reduced pressure to obtain the alkaline aqueous layer, which was acidified (to pH = 1) with a dropwise addition of 1.5 M HCl to get a white precipitate. The residue was collected by centrifugation, washed with (3 × 40 mL) distilled water and (2 × 40 mL) MeOH, and dried for 24 h under a vacuum at room temperature to obtain the final product as a light brown solid. Yield: 23 mg (56%).

Synthesis of polyMOFs. *Zn-poly(CPbdc-5a$_{0.27}$-CP).* To an 8-dram scintillation glass vial (with a Teflon-lined cap), poly(CPbdc-5a$_{0.27}$-CP) (7 mg, 0.034 μmol reactive CPbdc-5a units), $Zn(NO_3)_2{\cdot}6H_2O$ (48 mg, 0.18 mmol), and 1 mL of DMF were added. The vial was then transferred to an isothermal oven and heated at 100 °C for 24 h. Yield: 6 mg (80% w.r.t poly(CPbdc-5a$_{0.27}$-CP)). A similar procedure was followed to obtain Zn-poly(CPbdc-5a$_{0.27}$-CP) at 60 and 80 °C, respectively, by heating the polymer solution at 60 and 80 °C, respectively.

Zn-poly(CPbdc-2a$_{0.28}$-CP). To an 8-dram scintillation glass vial, poly(CPbdc-2a$_{0.28}$-CP) (7 mg, 0.035 μmol reactive CPbdc-2a units), $Zn(NO_3)_2{\cdot}6H_2O$ (48 mg, 0.18 mmol), and 1 mL of DMF were added. The vial was then transferred to an isothermal oven and heated at 100 °C for 24 h. Yield: 5 mg (70% w.r.t poly(CPbdc-2a$_{0.28}$-CP)). The same procedure was followed to obtain Zn-poly(CPbdc-2a$_{0.17}$-CP) and Zn-poly-(CPbdc-2a$_{0.26}$-CP-CPOH$_{0.11}$).

RESULTS AND DISCUSSIONS

Synthesis and Characterization of Polymeric Linkers. Inspired by the polymeric linker structure of Yazaki et al.,[2] dimethyl 2-(2-(cyclopent-3-en-1-ylmethoxy)ethoxy)-terephthalate (CPbdc-5e; CP = cyclopentene; "e" = the ester form of H_2bdc; "5" = the number of methylene units and oxygen atoms between the CP unit and H_2bdc-ester moiety) was initially designed starting from 3-cyclopentene-1-carboxylic acid using a multistep procedure (Figures S1−S5). For polymerization, a mixture of 200 equiv of CPbdc-5e and 150 equiv of CP (as a comonomer) was combined with 1 equiv of the G3 catalyst at 0 °C for 60 min, followed by quenching with ethyl vinyl ether, resulting in a pale brown viscous polymer (Figure S6). The ester polymer was hydrolyzed using KOH in a water:THF mixture to afford the desired random copolymer ligand, poly(CPbdc-5a$_{0.27}$−CP) (where "a" = the acid form of H_2bdc). ^{1}H NMR spectra show the emergence of characteristic proton signals corresponding to CP and CPbdc-5a repeating units with no traces of residual monomers (Figure S7). The relative proton peak integration revealed an incorporation of 27% of CPbdc-5a in the copolymer, with the remaining 73% being CP units, producing a random copolymer. The number-average molecular weight of poly(CPbdc-5a$_{0.27}$-CP) was evaluated using gel permeation chromatography (GPC), which gave a value of $M_{n,GPC}$ = 54 710 g mol^{-1} and a narrow $Đ$ of 1.41 (Figure S8 and Table S1).

To probe the effect of the spacer length in producing polyMOFs, dimethyl 2-(cyclopent-3-en-1-ylmethoxy)-terephthalate (CPbdc-2e) was synthesized, copolymerized with CP using G3 (Figures 1 and S8−S11), and hydrolyzed to produce poly(CPbdc-2a$_{0.28}$-CP) with a comparable loading (∼28%) of H_2bdc pendants and an $M_{n,GPC}$ value of 55 190 g mol^{-1} ($Đ$ = 1.26).

Cyclopentenes are significantly less strained and favor lower temperatures (0 °C) to polymerize to higher molecular weights and narrow $Đ$.[18] The lower ring strain of cyclopentene derivatives promotes the depolymerization of poly-(pentenamer)s at room (or higher) temperatures and/or under dilute conditions in the presence of Grubbs catalysts.[11,19] G3 typically promotes rapid depolymerization of poly(pentenamer)s at room temperature (25 °C)[11]; thus, all the ester-derived polymers were synthesized under neat monomer conditions (i.e., without solvents) at 0 °C. Attempts to homopolymerize CPbdc-5e or CPbdc-2e using G3 at 0 °C yielded no polymers, likely due to practical limitations in running the reaction. For instance, both the CPbdc derivatives were too viscous and were difficult to stir with a stir bar after ∼5 min at 0 °C, constraining the initiator solubility in the reaction mixture and hindering initiation and propagation.[19] Thus, to obtain polymers with H_2bdc pendant ligands, less viscous CP was chosen as the comonomer to serve as a "reactive diluent" to improve the mixing of the reaction components as well as the polymerization reaction. The volume of CP was kept to a minimum (∼40−50 μL, see the Experimental Methods section) that was sufficient to mix other components and stir at 0 °C to produce polymers with a reasonable (∼25−28%) composition of CPbdc repeating units. Increasing the feed content of CP resulted in polymer chains

https://doi.org/10.1021/acs.chemmater.4c01794
Chem. Mater. 2024, 36, 9696−9703

with more CP units and a reduced percentage of CPbdc, which ultimately affected their ability to form polyMOFs (vide infra).

Synthesis and Characterization of polyMOFs. Using standard solvothermal methods for IRMOF-1 synthesis, poly(CPbdc-5a$_{0.27}$-CP) was combined with Zn(II) in DMF and heated at 100 °C for 24 h to afford pale yellow microcrystalline solids (Figure S12). This microcrystalline material, assigned as Zn-poly(CPbdc-5a$_{0.27}$-CP), was characterized by PXRD, which produced a pattern of reflections consistent with that for IRMOF-1, indicating the assembly of the desired polyIRMOF-1 material (Figure 3a,b). A broad feature in the PXRD at $2\theta \sim 20°$ suggests a degree of amorphous content in Zn-poly(CPbdc-5a$_{0.27}$-CP) that may originate from the underlying polymer ligand.

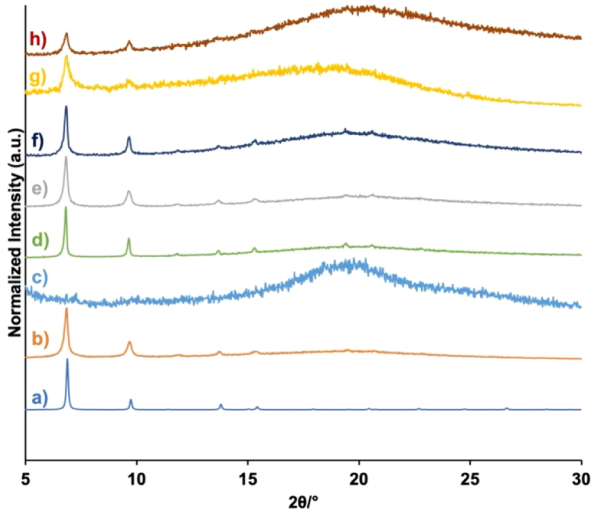

Figure 3. PXRD pattern of a) IRMOF-1 (simulated), b) Zn-poly(CPbdc-5a$_{0.27}$-CP), c) poly(CPbdc-5a$_{0.27}$-CP), d) Zn-poly-(CPbdc-2a$_{0.28}$-CP), e) Zn-poly(CPbdc-5a$_{0.25}$-CP-CPOH$_{0.15}$), f) Zn-poly(CPbdc-2a$_{0.26}$-CP-CPOH$_{0.11}$), g) Zn-poly(CPbdc-5a$_{0.14}$-CP-CPOH$_{0.15}$), and h) Zn-poly(CPbdc-2a$_{0.17}$-CP).

Attempts to synthesize Zn-poly(CPbdc-5a$_{0.27}$-CP) at lower temperatures (e.g., 60 and 80 °C) produced materials with PXRD patterns similar to the polyMOF produced at 100 °C (Figure S13). However, a reduction in peak intensity at lower angles, a relatively noisy baseline, and a more prominent, broad feature at $2\theta \sim 20°$ for the polyMOF analogs, specifically for Zn-poly(CPbdc-5a$_{0.27}$-CP) at 60 °C, indicated that the synthesis at 100 °C gave more crystalline polyMOFs. For the remainder of the study, unless specifically mentioned, Zn-poly(CPbdc-5a$_{0.27}$-CP) denotes the polyMOF analogue obtained at 100 °C.

The PXRD pattern of poly(CPbdc-5a$_{0.27}$-CP) expectedly exhibited no reflections and was amorphous with a broad feature centered at $2\theta \sim 20°$ (Figure 3c). To further ensure the crystallinity origin of Zn-poly(CPbdc-5a$_{0.27}$-CP), a control study was also performed by combining Zn(II) with the ester version of the poly(CPbdc-5a$_{0.27}$-CP) ligand (i.e., poly(CPbdc-5e$_{0.27}$-CP)); no solid materials were produced with the ester polymer ligand precursor and Zn(II) (Figure S14). The contents of this control reaction were evaluated by PXRD by drop casting ~10 μL of the reaction solution onto a sample plate and partially air-dried. The resulting film did not produce any sharp reflections, with only a broad feature at $2\theta \sim 20°$. The SEM image of the material showed a featureless, film-like morphology with no characteristics of a polyMOF (Figure S14).

To examine ambient stability, DMF-wetted Zn-poly(CPbdc-5a$_{0.27}$-CP) was stored in air, and the PXRD pattern was recorded after its exposure for 1 day and 1 week (Figure S15). The PXRD pattern remained somewhat preserved, with no notable shift of the peak position or reduction in peak intensity; however, after ambient storage for 1 day and 1 week, there was significant peak broadening compared to the original PXRD pattern. By contrast, IRMOF-1 (based on the molecular H_2bdc linker) collapses and shows a complete loss of PXRD reflections after exposure to air for just 1 day.[20]

Applying the same experimental protocol (to obtain Zn-poly(CPbdc-5a$_{0.27}$-CP)), poly(CPbdc-2a$_{0.28}$-CP) was combined with Zn(II) to obtain Zn-poly(CPbdc-2a$_{0.28}$-CP) as a white-to-pale yellow microcrystalline powder (Figure S12). The PXRD pattern of Zn-poly(CPbdc-2a$_{0.28}$-CP) showed reflections consistent with the pattern of Zn-poly(CPbdc-5a$_{0.27}$-CP) (Figure 3d), indicating the assembly of poly-(CPbdc-2a$_{0.28}$-CP) into a polyMOF with an IRMOF-like structure.

SEM imaging revealed that the Zn-poly(CPbdc-5a$_{0.27}$-CP) particles were generally spherical, intergrown, and possessed a complex, hierarchical surface morphology (Figure 4). This

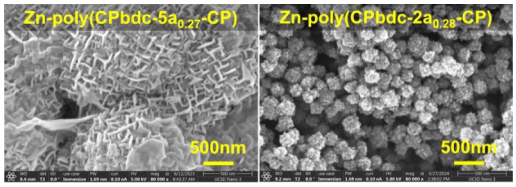

Figure 4. SEM images of Zn-poly(CPbdc-5a$_{0.27}$-CP) (left) and Zn-poly(CPbdc-2a$_{0.28}$-CP) (right) (scale bar = 500 nm).

unusual morphology is similar to those observed for some other polyMOFs.[16,21−23] Synthesis temperatures notably influenced the morphology of the Zn-poly(CPbdc-5a$_{0.27}$-CP) particles. Zn-poly(CPbdc-5a$_{0.27}$-CP) synthesized at 60 °C showed round particles with a relatively smooth surface, whereas Zn-poly(CPbdc-5a$_{0.27}$-CP) produced at 80 °C showed a surface morphology similar to that of Zn-poly(CPbdc-5a$_{0.27}$-CP) synthesized at 100 °C, but with a greater content of amorphous polymer chains enwrapping the crystalline particles (as indicated in Figure S16). The morphological results of these polyMOFs corroborate with their corresponding PXRD patterns for sharper reflections of Zn-poly(CPbdc-5a$_{0.27}$-CP) and Zn-poly(CPbdc-5a$_{0.27}$-CP)/80 °C that produced spherical particles with complex, hierarchical surfaces, whereas less crystalline Zn-poly(CPbdc-5a$_{0.27}$-CP)/60 °C was obtained as rounded solids. Interestingly, Zn-poly(CPbdc-2a$_{0.28}$-CP) particles yielded quasi-spherical clusters of intergrown crystallites that were different from Zn-poly(CPbdc-5a$_{0.27}$-CP) morphology (Figure 4), suggesting that the spacer length also markedly affects the structural morphology of the resultant polyMOFs.

The ATR-IR spectra of several samples were collected to better characterize the materials. The ATR-IR spectrum of poly(CPbdc-5a$_{0.27}$-CP) was obtained, which showed asymmetric and symmetric carbonyl (>CO) stretches of the terephthalate units (bdc) at 1690 and 1430 cm^{-1}, respectively. By comparison, the same stretches in the polyMOF Zn-poly(CPbdc-5a$_{0.27}$-CP) exhibit bands at 1595 and 1385 cm^{-1}, which are red-shifted compared to the corresponding free

https://doi.org/10.1021/acs.chemmater.4c01794
Chem. Mater. 2024, 36, 9696−9703

polymer ligand and indicate coordination to Zn(II). The red-shifts of the carbonyl groups are consistent with previously reported IR data for IRMOF-1 materials, where the asymmetric >CO stretching band of the uncoordinated molecular H_2bdc linker (1680 cm^{-1}) is red-shifted (1563 cm^{-1}) in the MOF.[24−26] A similar red shift was observed for the asymmetric (1584 cm^{-1}) and symmetric (1379 cm^{-1}) carbonyl stretches of Zn-poly(CPbdc-2$a_{0.28}$-CP) compared to the free polymer ligand poly(CPbdc-2$a_{0.28}$-CP) (asymmetric 1684 cm^{-1} and symmetric 1429 cm^{-1}).

Zn-poly(CPbdc-5$a_{0.27}$-CP) and Zn-poly(CPbdc-2$a_{0.28}$-CP) were activated (vide infra) and dissolved in a 2 M HCl/DMF mixture, precipitated in water, washed with water and MeOH, and dried under a vacuum to isolate their corresponding polymer ligands and confirm the structural and chemical integrity of the polymer ligand after polyMOF synthesis (relative to their pristine form; see the Supporting Information). ^{1}H NMR spectroscopy and GPC analysis results of the reisolated polymers showed that they were essentially unchanged from their original forms (Figures S8 and S18 and Table S1). This demonstrates that the poly(pentenamer)s were sufficiently stable during the MOF synthesis, excluding the possibility that degradation to monomers or oligomers is responsible for polyMOF formation. More importantly, the recombination of the recovered polymeric linker (poly(CPbdc-5$a_{0.27}$-CP)) with zinc nitrate hexahydrate under the same reaction conditions resulted in polyMOF materials with identical PXRD patterns compared to the originally prepared, pristine Zn-poly(CPbdc-5$a_{0.27}$-CP) samples (Figure S19).

To further verify the versatility of the ROMP approach, a CP monomer with a pendant hydroxymethyl group (3-cyclopenten-1-ylmethanol, CPOH) was included in the polymerization to generate a random terpolymer ligand (poly(CPbdc-5$a_{0.25}$-CP-CPOH$_{0.15}$)) with a composition of 15% CPOH, 25% CPbdc-5a, and 60% CP (Figure S20). A second terpolymer ligand was synthesized using CPbdc-2e with CP and CPOH to generate poly(CPbdc-2$a_{0.26}$-CP-CPOH$_{0.11}$) (Figure S21). These new polymer ligands were used to prepare IRMOF-like networks under standard synthetic conditions at 100 °C. The resulting Zn-poly(CPbdc-5$a_{0.25}$-CP-CPOH$_{0.15}$) and Zn-poly(CPbdc-2$a_{0.26}$-CP-CPOH$_{0.11}$) were characterized using PXRD (Figure 3e,f) and SEM imaging (Figure 5), which revealed that both terpolymers also formed the desired polyMOF structures.

To evaluate the effect of comonomer composition, a third polymer ligand was prepared, poly(CPbdc-5$a_{0.14}$-CP-CPOH$_{0.15}$). Importantly, a notable loss in the crystallinity of the polyMOF (Zn-poly(CPbdc-5$a_{0.14}$-CP-CPOH$_{0.15}$)) was observed, as gauged by PXRD (Figures 3g and S22), as the percentage of CPbdc-5a was reduced from 25% to 14% in the polymer linker. To verify this observation, the loading percentage of the H_2bdc units was reduced in one of the simpler copolymers of CPbdc-2a and CP; the resulting polymer, poly(CPbdc-2$a_{0.17}$-CP), was combined with Zn(II) to produce Zn-poly(CPbdc-2$a_{0.17}$-CP) as a gel (Figures S23 and S24), rather than as a microcrystalline solid. The PXRD pattern of Zn-poly(CPbdc-2$a_{0.17}$-CP) showed a few low-angle reflections (at $2\theta \sim 6.8°$ and 9.7°) consistent with the IRMOF-1 lattice but contained a broad intense feature positioned at $2\theta \sim 20°$, indicating that a large proportion of the material is amorphous (Figure 3h). These findings suggest that some minimum proportion ($\gtrsim$25%) of H_2bdc repeating units is necessary to produce a highly crystalline polyMOF.

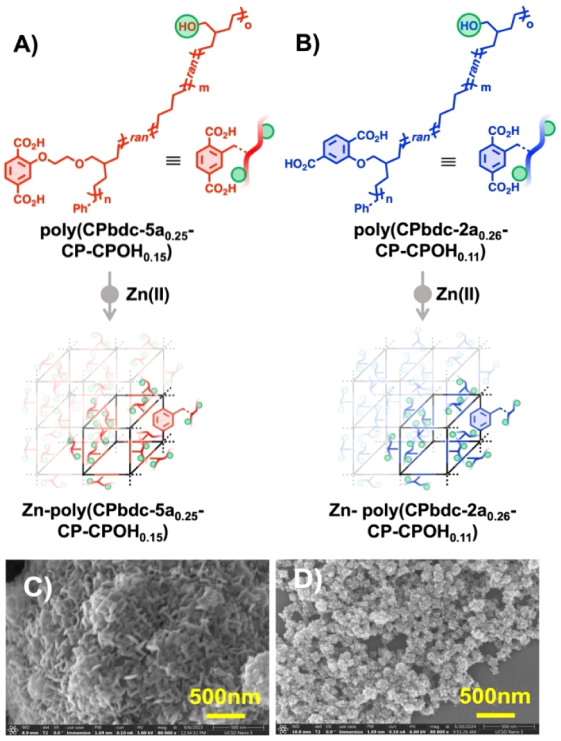

Figure 5. A) Synthesis of Zn-poly(CPbdc-5$a_{0.25}$-CP-CPOH$_{0.15}$) and B) Zn-poly(CPbdc-2$a_{0.26}$-CP-CPOH$_{0.11}$) under solvothermal conditions from poly(CPbdc-5$a_{0.25}$-CP-CPOH$_{0.15}$) and poly(CPbdc-2$a_{0.26}$-CP-CPOH$_{0.11}$), respectively. SEM images of C) Zn-poly(CPbdc-5$a_{0.25}$-CP-CPOH$_{0.15}$) and D) Zn-poly(CPbdc-2$a_{0.26}$-CP-CPOH$_{0.11}$).

N_2 Gas Sorption Behavior of the polyMOFs. Dinitrogen (N_2) physisorption experiments were performed on Zn-poly(CPbdc-5$a_{0.27}$-CP) at 77 K following activation by washing the solids repeatedly with fresh DMF, exchanging the solvent for methylene chloride (CH_2Cl_2), and vacuum drying at 105 °C for 10 h. A type IV (a) isotherm profile was observed, showing significant adsorption by mesopores (a pore width of 2−50 nm) and modest adsorption by micropores (a pore width of <2 nm) (Figures 6 and S25).[27] The BET surface area of Zn-poly(CPbdc-5$a_{0.27}$-CP) was found to be 124 ± 3 m^2 g^{-1}. Taking into account the mass fraction of the polymer in Zn-poly(CPbdc-5$a_{0.27}$-CP) (which does not contribute to porosity), the BET value can be normalized to 282 ± 8 m^2 g^{-1} (Table S2). The corrected value is much lower than that observed for native IRMOF-1 (up to 3800 m^2 g^{-1}),[28] indicating that the polymer chains are congested within the pores of Zn-poly(CPbdc-5$a_{0.27}$-CP), resulting in substantial pore-blocking, filling, and sealing effects throughout the material. Despite these limitations, Zn-poly(CPbdc-5$a_{0.27}$-CP) retains more porosity when compared to the polyMOF material reported by Yazaki et al.[2] Using lower synthesis temperatures to generate Zn-poly(CPbdc-5$a_{0.27}$-CP) (e.g., at 60 or 80 °C) resulted in much smaller or no measurable surface areas (Figure S26), consistent with their corresponding PXRD patterns and SEM data.

By contrast, 77 K N_2 sorption by Zn-poly(CPbdc-2$a_{0.28}$-CP) after an identical sample treatment showed greatly enhanced micropore adsorption while retaining the overall type IV (a) isotherm profile (Figure 6). The BET surface area of Zn-poly(CPbdc-2$a_{0.28}$-CP) was found to be 557 ± 22 m^2 g^{-1}, with

https://doi.org/10.1021/acs.chemmater.4c01794
Chem. Mater. 2024, 36, 9696−9703

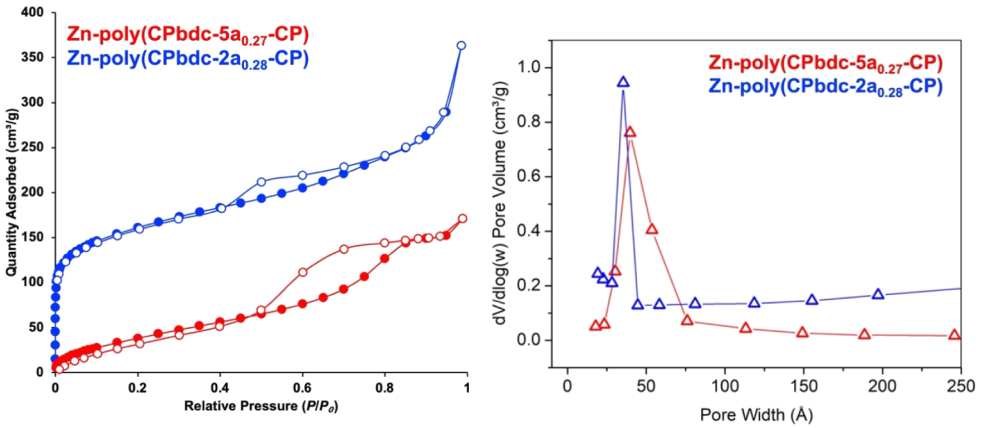

Figure 6. N_2 physisorption isotherm (left) and BJH pore size distribution (right) plots of Zn-poly(CPbdc-$5a_{0.27}$-CP) (red) and Zn-poly(CPbdc-$2a_{0.28}$-CP) (blue).

a corresponding mass-corrected value of 1151 ± 45 m^2 g^{-1}. These values are comparable to archetypal porous polyMOFs with ligand units in the polymer backbone, such as polyIRMOF-1 (230−1100 m^2 g^{-1})[16] and polyUiO-66 (200−400 m^2 g^{-1}),[29] and show that high porosity is accessible in Zn-poly(CPbdc-$2a_{0.28}$-CP). A Horvath−Kawazoe treatment of adsorption data shows that Zn-poly(CPbdc-$2a_{0.28}$-CP) has a median pore width of 6.5 Å, which agrees well with previous measurements on functionalized IRMOF materials.[30] Zn-poly(CPbdc-$2a_{0.28}$-CP) displays a significantly greater micropore volume compared to Zn-poly(CPbdc-$5a_{0.27}$-CP) (0.23 cm^3/g vs 0.05 cm^3/g at pore widths of ca. 2 nm, Figure S25). The smaller-spaced CPbdc-2a repeating units in poly(CPbdc-$2a_{0.28}$-CP) likely reduce the degree of crowding of polymer chains into or surrounding the polyMOF pores, which reduces pore-blocking and improves the porosity of Zn-poly(CPbdc-$2a_{0.28}$-CP) when compared to Zn-poly(CPbdc-$5a_{0.27}$-CP).

The desorption profiles of both materials show hysteresis between P/P_0 = 0.45 and 0.85, resembling type H2 hysteresis in the IUPAC classification.[27] The contribution of mesopores to the porosity in both cases is observable using pore size distributions determined by the Barrett−Joyner−Halenda (BJH) method (Figure 6), which show mesopores of widths centered around 40 and 35 Å for Zn-poly(CPbdc-$5a_{0.27}$-CP) and Zn-poly(CPbdc-$2a_{0.28}$-CP), respectively. These pores are not intrinsic to individual crystallites of Zn-poly(CPbdc-$5a_{0.27}$-CP) and are attributed to hierarchical mesopores formed by the packing of crystallites into aggregates, as seen in the SEM images of both materials (Figure 4).

CONCLUSIONS

In summary, a new strategy is reported to generate porous, crystalline polyMOFs using tailor-made poly(pentenamer)s containing H_2bdc units as pendants. Synthesis of polymer ligands using ROMP provides access to control their composition and *Đ*. These poly(pentenamer)s were assembled with Zn(II) to produce polyMOFs with IRMOF-like structures. The degree of crystallinity of the polyMOFs was notably improved by increasing the content of H_2bdc pendant ligands in the poly(pentenamer) chain, which can be controlled by simply adjusting the feed content of the (co)monomers during polymerization. The use of ROMP also allowed for the synthesis of random terpolymers with a specific loading of hydroxymethyl dangling units (alongside H_2bdc pendants) that readily assembled into IRMOF-like polyMOFs. The polyMOFs based on the poly(pentenamer) linkers with a shorter spacer length were morphologically distinctive and significantly more porous compared with their counterparts with longer-spaced side chain ligands. Given the widespread use of ROMP, the availability of structurally diverse alkenamers, and accessibility to side chain engineering of polymers, we believe this approach will prove to be a major advancement in obtaining crystalline, porous polyMOFs with tailored properties.

ASSOCIATED CONTENT

Supporting Information

The Supporting Information is available free of charge at https://pubs.acs.org/doi/10.1021/acs.chemmater.4c01794.

Synthesis and characterization of monomers and polymers; polyMOF synthesis procedures and characterization; summary of GPC analysis of all polymers (Table 1); summary of the BET surface area mass adjustment (Table S2); ^{1}H and ^{13}C NMR spectra of CPOH, 2-(cyclopent-3-en-1-ylmethoxy)acetic acid, 2-(cyclopent-3-en-1-ylmethoxy)ethan-1-ol, 2-(cyclopent-3-en-1-ylmethoxy)ethyl 4-methylbenzenesulfonate, and CPbdc-5e (Figures S1−S5); pictorial demonstration of the experimental setup (Figure S6); ^{1}H NMR spectra of poly(CPbdc-$5a_{0.27}$-CP), poly(CPbdc-$2a_{0.28}$-CP), and poly(CPbdc-$5a_{0.25}$-CP-$CPOH_{0.15}$) (Figures S7, S11, S18, and S20−S23); GPC elution curves (Figure S8); ^{1}H and ^{13}C NMR spectra of cyclopent-3-en-1-ylmethyl 4-methylbenzenesulfonate and CPbdc-2e (Figures S9 and S10); pictures of the DMF-wetted microcrystalline materials (Figure S12); PXRD patterns of Zn-poly-(CPbdc-$5a_{0.27,}$-CP) (Figures S13, S15, and S19); picture, SEM image, and PXRD pattern of the product (Figure S14); SEM images of Zn-poly(CPbdc-$5a_{0.27}$-CP) (Figure S16); ATR-IR spectra (Figure S17); images of Zn-poly(CPbdc-$2a_{0.17}$-CP) (Figure S24); Horvath−Kawazoe pore volume and dV/dw plots (Figure S25); N_2 gas sorption isotherm and BJH pore size distribution plots (Figure S26) (PDF)

AUTHOR INFORMATION

Corresponding Author

Seth M. Cohen − *Department of Chemistry and Biochemistry, University of California, San Diego, La Jolla, California*

https://doi.org/10.1021/acs.chemmater.4c01794
Chem. Mater. 2024, 36, 9696−9703

92093, United States; orcid.org/0000-0002-5233-2280; Email: scohen@ucsd.edu

Authors

Prantik Mondal − *Department of Chemistry and Biochemistry, University of California, San Diego, La Jolla, California 92093, United States;* orcid.org/0000-0002-4236-6815

Debobroto Sensharma − *Department of Chemistry and Biochemistry, University of California, San Diego, La Jolla, California 92093, United States;* orcid.org/0000-0002-4918-0730

Complete contact information is available at: https://pubs.acs.org/10.1021/acs.chemmater.4c01794

Author Contributions

The manuscript was written through the contributions of all authors. All authors have given approval to the final version of the manuscript. P.M. and S.M.C. designed the materials and experimental strategy; P.M. conducted the experiments; D.S. evaluated the gas sorption behavior of the materials; P.M., D.S., and S.M.C. wrote the manuscript; P.M. and S.M.C. supervised the editing and writing of this manuscript. All authors have given approval to the final version of the manuscript.

Notes

The authors declare no competing financial interest.

■ ACKNOWLEDGMENTS

This work was supported by the Department of Energy, Office of Basic Energy Sciences, Division of Materials Science and Engineering (under Award No. DE-FG02-08ER46519). We thank Dr. Yongxuan Su for the mass spectrometry sample analysis at the Molecular Mass Spectrometry Facility at U.C. San Diego. This work was performed in part at the San Diego Nanotechnology Infrastructure (SDNI) of U.C. San Diego, a member of the National Nanotechnology Coordinated Infrastructure, which is supported by the National Science Foundation (Grant ECCS-2025752).

■ REFERENCES

(1) Caire da Silva, L.; Rojas, G.; Schulz, M. D.; Wagener, K. B. Acyclic diene metathesis polymerization: History, methods and applications. *Prog. Polym. Sci.* **2017**, *69*, 79−107.

(2) Yazaki, K.; Takahashi, M.; Miyajima, N.; Obata, M. Construction of a polyMOF using a polymer ligand bearing the benzenedicarboxylic acid moiety in the side chain. *New J. Chem.* **2020**, *44* (14), 5182−5185.

(3) Aoshima, S.; Kanaoka, S. A Renaissance in Living Cationic Polymerization. *Chem. Rev.* **2009**, *109* (11), 5245−5287.

(4) Binder, W. H.; Zirbs, R. Allyl- and Hydroxytelechelic Poly(isobutylenes). In *Materials Syntheses: A Practical Guide*, Schubert, U.; Hüsing, N.; Laine, R. M., Eds.; Springer Vienna, 2008. pp. 209216.

(5) Kottisch, V.; O'Leary, J.; Michaudel, Q.; Stache, E. E.; Lambert, T. H.; Fors, B. P. Controlled Cationic Polymerization: Single-Component Initiation under Ambient Conditions. *J. Am. Chem. Soc.* **2019**, *141* (27), 10605−10609.

(6) Grubbs, R. B.; Grubbs, R. H. 50th Anniversary Perspective: Living Polymerization—Emphasizing the Molecule in Macromolecules. *Macromolecules* **2017**, *50* (18), 6979−6997.

(7) Hadjichristidis, N.; Pitsikalis, M.; Iatrou, H.; Sakellariou, G. Macromolecular Architectures by Living and Controlled/Living Polymerizations. In *Controlled and Living Polymerizations: From mechanisms to Applications*; Matyjaszewski, K.; Muller, A. H. E., Eds.; Wiley, 2009. pp. 343443. DOI: .

(8) Pearson, M. A.; Dincă, M.; Johnson, J. A. Radical PolyMOFs: A Role for Ligand Dispersity in Enabling Crystallinity. *Chem. Mater.* **2021**, *33* (24), 9508−9514.

(9) Bielawski, C. W.; Grubbs, R. H. Living ring-opening metathesis polymerization. *Prog. Polym. Sci.* **2007**, *32* (1), 1−29.

(10) Orski, S. V.; Kassekert, L. A.; Farrell, W. S.; Kenlaw, G. A.; Hillmyer, M. A.; Beers, K. L. Design and Characterization of Model Linear Low-Density Polyethylenes (LLDPEs) by Multidetector Size Exclusion Chromatography. *Macromolecules* **2020**, *53* (7), 2344−2353.

(11) Neary, W. J.; Kennemur, J. G. Polypentenamer Renaissance: Challenges and Opportunities. *ACS Macro Lett.* **2019**, *8* (1), 46−56.

(12) Mandal, I.; Mandal, A.; Rahman, M. A.; Kilbinger, A. F. M. Chain transfer agents for the catalytic ring opening metathesis polymerization of norbornenes. *Chem. Sci.* **2022**, *13* (42), 12469−12478.

(13) Wolf, W. J.; Lin, T.-P.; Grubbs, R. H. Examining the Effects of Monomer and Catalyst Structure on the Mechanism of Ruthenium-Catalyzed Ring-Opening Metathesis Polymerization. *J. Am. Chem. Soc.* **2019**, *141* (44), 17796−17808.

(14) Yasir, M.; Liu, P.; Tennie, I. K.; Kilbinger, A. F. M. Catalytic living ring-opening metathesis polymerization with Grubbs' second- and third-generation catalysts. *Nat. Chem.* **2019**, *11* (5), 488−494.

(15) Albagli, D.; Bazan, G.; Wrighton, M. S.; Schrock, R. R. Well-defined redox-active polymers and block copolymers prepared by living ring-opening metathesis polymerization. *J. Am. Chem. Soc.* **1992**, *114* (11), 4150−4158.

(16) Zhang, Z.; Nguyen, H. T. H.; Miller, S. A.; Cohen, S. M. polyMOFs: A Class of Interconvertible Polymer-Metal-Organic-Framework Hybrid Materials. *Angew. Chem., Int. Ed.* **2015**, *54* (21), 6152−6157.

(17) Tanabe, K. K.; Allen, C. A.; Cohen, S. M. Photochemical Activation of a Metal−Organic Framework to Reveal Functionality. *Angew. Chem., Int. Ed.* **2010**, *49* (50), 9730−9733.

(18) Hlil, A. R.; Balogh, J.; Moncho, S.; Su, H.-L.; Tuba, R.; Brothers, E. N.; Al-Hashimi, M.; Bazzi, H. S. Ring opening metathesis polymerization (ROMP) of five- to eight-membered cyclic olefins: Computational, thermodynamic, and experimental approach. *J. Polym. Sci., Part A: Polym. Chem.* **2017**, *55* (18), 3137−3145.

(19) Song, K.; Kim, K.; Hong, D.; Kim, J.; Heo, C. E.; Kim, H. I.; Hong, S. H. Highly active ruthenium metathesis catalysts enabling ring-opening metathesis polymerization of cyclopentadiene at low temperatures. *Nat. Commun.* **2019**, *10* (1), 3860.

(20) Nguyen, J. G.; Cohen, S. M. Moisture-Resistant and Superhydrophobic Metal−Organic Frameworks Obtained via Post-synthetic Modification. *J. Am. Chem. Soc.* **2010**, *132* (13), 4560−4561.

(21) Qiu, S.; Xue, M.; Zhu, G. Metal−organic framework membranes: From synthesis to separation application. *Chem. Soc. Rev.* **2014**, *43* (16), 6116−6140.

(22) Ayala, S.; Bentz, K. C.; Cohen, S. M. Block co-polyMOFs: Morphology control of polymer−MOF hybrid materials. *Chem. Sci.* **2019**, *10* (6), 1746−1753.

(23) Mileo, P. G. M.; Yuan, S.; Ayala, S., Jr.; Duan, P.; Semino, R.; Cohen, S. M.; Schmidt-Rohr, K.; Maurin, G. Structure of the Polymer Backbones in polyMOF Materials. *J. Am. Chem. Soc.* **2020**, *142* (24), 10863−10868.

(24) Cho, W.; Lee, H. J.; Oh, M. Growth-Controlled Formation of Porous Coordination Polymer Particles. *J. Am. Chem. Soc.* **2008**, *130* (50), 16943−16946.

(25) Zhang, Z.; Chen, Y.; Xu, X.; Zhang, J.; Xiang, G.; He, W.; Wang, X. Well-Defined Metal−Organic Framework Hollow Nanocages. *Angew. Chem., Int. Ed.* **2014**, *53* (2), 429−433.

(26) Hadjiivanov, K. I.; Panayotov, D. A.; Mihaylov, M. Y.; Ivanova, E. Z.; Chakarova, K. K.; Andonova, S. M.; Drenchev, N. L. Power of Infrared and Raman Spectroscopies to Characterize Metal-Organic Frameworks and Investigate Their Interaction with Guest Molecules. *Chem. Rev.* **2021**, *121* (3), 1286−1424.

(27) Thommes, M.; Kaneko, K.; Neimark, A. V.; Olivier, J. P.; Rodriguez-Reinoso, F.; Rouquerol, J.; Sing, K. S. W. Physisorption of gases, with special reference to the evaluation of surface area and pore size distribution (IUPAC Technical Report). *Pure Appl. Chem.* **2015**, *87* (9−10), 1051−1069.
(28) Kaye, S. S.; Dailly, A.; Yaghi, O. M.; Long, J. R. Impact of Preparation and Handling on the Hydrogen Storage Properties of Zn4O(1,4-benzenedicarboxylate)3 (MOF-5). *J. Am. Chem. Soc.* **2007**, *129* (46), 14176−14177.
(29) Ayala, S.; Zhang, Z.; Cohen, S. M. Hierarchical structure and porosity in UiO-66 polyMOFs. *Chem. Commun.* **2017**, *53* (21), 3058−3061.
(30) Allen, C. A.; Boissonnault, J. A.; Cirera, J.; Gulland, R.; Paesani, F.; Cohen, S. M. Chemically crosslinked isoreticular metal−organic frameworks. *Chem. Commun.* **2013**, *49* (31), 3200−3202.

https://doi.org/10.1021/acs.chemmater.4c01794
Chem. Mater. 2024, 36, 9696−9703